Boundary Element Analysis of a Trapezoidal Transmission Line

Brent Toland and Tatsuo Itoh, *Fellow, IEEE*

Abstract— **A full wave analysis of a transmission line with a trapezoidal cross section is described. The boundary element method (BEM) is used; and by making a convenient choice for the dyadic Green's function, the method is shown to be very efficient in comparison to appropriate alternative methods of analysis. Further, in this application, it is shown that for electrically small dimensions, spurious solutions are suppressed by the selection of integral equations. Finally, the analysis is verified by comparisons to calculated results from a vector finite element computer program, and some dispersion data are presented.**

I. Introduction

In order to design more compact MMIC's, thin film microstrip transmission lines have been investigated [1], [2]. These transmission lines have a narrow width conductor over a thin, layered dielectric of polyimide, which substantially reduces the circuit size. Unfortunately, these structures have greater transmission losses than conventional MMIC's. It is therefore necessary to develop transmission lines which have lower losses than the narrow width microstrip lines. Recently, a few structures have been proposed in order to achieve this goal [2]. These structures attempt to reduce the conductor losses by reducing the currents on the strip conductor. This is accomplished in [2] by using some novel transmission line cross sections (i.e., trapezoids or V-shaped strip conductors). We have selected for analysis the trapezoidal cross section [see Fig. 1(a)] because it gives the lowest conductor loss of the structures investigated in [2].

Since the trapezoidal line has only recently been proposed, there are no published full wave analyses. It is the purpose of this paper to present one here. First, we note that the trapezoidal geometry does not lend itself easily to most conventional methods of analysis. Since this structure is similar to the Microslab waveguide proposed in [3], a mode-matching approach is possible, although this would require that the slanted sides be modeled in a staircase fashion, and heavy computation would be involved to obtain an approximate result. Perhaps a more expedient choice would be to use the Finite Element Method (FEM), which has become quite popular over the past two decades. Instead, we have chosen to use the Boundary Element Method (BEM) to analyze this structure. This method has also had increasing popularity in recent years [4]–[9]. The BEM has the advantage that integral equations are formed only along the boundaries between different dielectric regions, as opposed to over the entire cross section of the structure as in the FEM. This results in a significant decrease in the number of basis functions required to accurately solve for the propagation constant. In addition, the BEM can handle open regions as easily as closed regions simply by making an obvious choice for the Green's function. On the other hand, some care must be taken in applying the FEM, because the FEM mesh must be terminated so that the imposed boundary does not affect the accuracy of the solution. This may also require increased computation, because the size of the chosen cross section must either be large enough to model the open structure, or some other method of mesh termination must be chosen [10], [11]. In addition, to further enhance the BEM for our application, the electric and magnetic Green's functions are chosen so that the integration over the ground plane is not necessary. This reduces the problem to a line integral over the contour Γ_{abcd} [for the infinitely thin strip, see Fig. 1(b)]. With all this in mind, it is apparent that the BEM possesses a computational advantage over the FEM for this application.

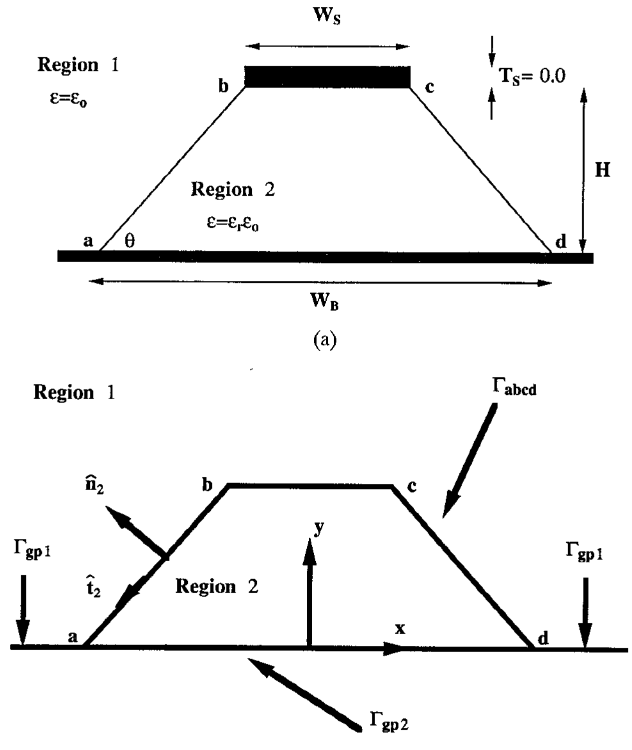

Fig. 1. Cross section of transmission line and coordinate systems used in BEM analysis.

Manuscript received April 17, 1992; revised October 26, 1992. This work was supported in part by the U.S. Army under Contract DAAL-03-88-K-0005 and by the ATR Optical and Radio Communications Research Laboratories.
IEEE Log Number 9206238.

II. Boundary Element Analysis

We begin with the following set of integral equations which can be found in many electromagnetics textbooks [12]:

$$\overline{E}(x',y') = \int_r [\overline{E}(x,y)\times\hat{n}] \cdot [\nabla\times\overline{\overline{G_e}}(x,y;x',y',\beta)]\,d\overline{r} - j\omega\mu_o \cdot \int_r [\overline{H}(x,y)\times\hat{n}]\cdot[\overline{\overline{G_e}}(x,y;x',y',\beta)]\,d\overline{r} \quad (1)$$

$$\overline{H}(x',y') = \int_r [\overline{H}(x,y)\times\hat{n}] \cdot [\nabla\times\overline{\overline{G_m}}(x,y;x',y',\beta)]\,d\overline{r} + j\omega\epsilon_r\epsilon_o \cdot \int_r [\overline{E}(x,y)\times\hat{n}]\cdot[\overline{\overline{G_m}}(x,y;x',y',\beta)]\,d\overline{r}. \quad (2)$$

The integrals are taken over the path Γ which encloses the homogeneous region "r" (in this paper, $r = 1, 2$). There are many possible choices for the electric Green's functions $\overline{\overline{G_e}}$ and the magnetic Green's functions $\overline{\overline{G_m}}$ [12], but here we choose the free space functions which obey the additional constraints of $\nabla\times\overline{\overline{G_m}}\times\hat{n} = 0$ and $\overline{\overline{G_e}}\times\hat{n} = 0$ on the ground plane $(x, y = 0)$. Here, $\hat{n}$ is out of the boundary. If we apply these conditions, the following forms for the Green's functions can be obtained (e.g., see [13, p. 66]):

$$\overline{\overline{G_e^r}} = \left[\overline{\overline{I}} - \frac{1}{k_r^2}\nabla\nabla'\right] f_e + 2\hat{y}\hat{y}g_o(\gamma_r R_i) \quad \text{and}$$
$$\overline{\overline{G_m^r}} = \left[\overline{\overline{I}} - \frac{1}{k_r^2}\nabla\nabla'\right] f_m - 2\hat{y}\hat{y}g_o(\gamma_r R_i) \quad (3)$$

for the electric and magnetic Green's functions, respectively. The terms f_e and f_m are defined as $f_e = g_o(\gamma_r R) - g_o(\gamma_r R_i)$ and $f_m = g_o(\gamma_r R) + g_o(\gamma_r R_i)$, respectively. We use the free-space Green's function in cylindrical coordinates, $g_o(\gamma_r R) = -(j/4)H_o^{(2)}(\gamma_r R)$, with

$$R = \sqrt{(x-x')^2 + (y-y')^2},$$
$$R_i = \sqrt{(x-x')^2 + (y+y')^2},$$
$$\gamma_r = \sqrt{k_r^2 - \beta^2}, \qquad k_r = \omega\sqrt{\mu_o\epsilon_o\epsilon_r}. \quad (4)$$

Here ϵ_r is the relative dielectric constant in region "r," $H_o^{(2)}(\gamma_r R)$ is the zero-order Hankel function of the second kind, and we have assumed $e^{-j\beta z}$ propagation.

The contour Γ depends on which region is enclosed (see Fig. 1). For region 1, Γ consists of the path along $abcd, \Gamma_{abcd}$, and the path along the ground plane, from point "a" to $x \to -\infty$ and from $x \to \infty$ back to "d," which we shall denote as Γ_{gp1}. In region 1, the argument of the Hankel function becomes imaginary, and hence as $R \to \infty$, there is no contribution from the path Γ_∞. This is the advantage of the BEM for the open structure. The contour for region 2 is over Γ_{abcd} (we are assuming an infinitely thin strip) and the ground plane path in region 2, Γ_{gp2}. Since the integrands are all zero on the ground plane, the integrals along this part of the contour can be eliminated, leaving only the contribution from Γ_{abcd}. By moving the observation point (x', y') to the boundary and performing several manipulations, these equations can be cast in the following form:

$$\frac{1}{2}M_t(x',y') = \int_r \left[-\frac{\partial f_e}{\partial n}\right] M_t(x,y) + \left[-\frac{\omega\mu_o\beta}{k_r^2}\frac{\partial f_e}{\partial t}\right] J_t(x,y) + \left[-\frac{j\omega\mu_o\gamma_r^2}{k_r^2} f_e\right] J_z(x,y)\,d\Gamma \quad (5)$$

$$\frac{1}{2}J_t(x',y') = \int_r \left[-\frac{\partial f_m}{\partial n}\right] J_t(x,y) + \left[-\frac{\omega\epsilon_r\epsilon_o\beta}{k_r^2}\frac{\partial f_m}{\partial t}\right] M_t(x,y) + \left[\frac{j\omega\epsilon_r\epsilon_o\gamma_r^2}{k_r^2} f_m\right] M_z(x,y)\,d\Gamma \quad (6)$$

$$\frac{1}{2}M_z(x',y') = \int_r \left[\frac{j\beta}{\gamma_r^2}\frac{\partial}{\partial t}\left\{\frac{\partial f_e}{\partial n'} - \frac{\partial f_m}{\partial n'}\right\}\right] M_t(x,y) + \left[-\frac{\partial f_m}{\partial n'}\right] M_z(x,y)\,d\Gamma + \int_r \left[\frac{j\omega\mu_o}{\gamma_r^2}\left\{\frac{\beta^2}{k_r^2}\frac{\partial^2 f_e}{\partial t\partial t'} + \frac{\partial^2 f_m}{\partial n\partial n'}\right\}\right] J_t(x,y) - \left[\frac{\beta}{\omega\epsilon_r}\frac{\partial f_e}{\partial t'}\right] J_z(x,y)\,d\Gamma \quad (7)$$

$$\frac{1}{2}J_z(x',y') = \int_r \left[\frac{j\beta}{\gamma_r^2}\frac{\partial}{\partial t}\left\{\frac{\partial f_m}{\partial n'} - \frac{\partial f_e}{\partial n'}\right\}\right] J_t(x,y) + \left[-\frac{\partial f_e}{\partial n'}\right] J_z(x,y)\,d\Gamma + \int_r \left[\frac{j\omega\epsilon_r\epsilon_o}{\gamma_r^2}\left\{\frac{\beta^2}{k_r^2}\frac{\partial^2 f_m}{\partial t\partial t'} + \frac{\partial^2 f_e}{\partial n\partial n'}\right\}\right] M_t(x,y) + \left[\frac{\beta}{\omega\mu_o}\frac{\partial f_m}{\partial t'}\right] M_z(x,y)\,d\Gamma. \quad (8)$$

In these equations, M_t and M_z are the tangential and axial directed components of the magnetic current $(\overline{M} = \overline{E}\times\hat{n})$ on the boundary, and J_t and J_z are the corresponding electric currents $(\overline{J} = \overline{H}\times\hat{n})$. These equations are valid on the boundary of each respected region, and can be combined and solved for the propagation constant as a function of frequency. The equations are made discrete by dividing the contour into segments, and then the unknown sources are expanded as piecewise constant basis functions. For example, for piecewise constant basis functions, we would have the sequence $M_t = [M_t(1), M_t(2), \cdots, M_t(N)]$, where there are N segments on the entire boundary Γ_{abcd}, and $M_t(j)$ is the value of M_t at the center of segment "j." We test the equations by point matching, and we obtain the following, for $i = 1, \cdots, N$:

$$\frac{1}{2}M_t(i) = \sum_{j=1}^{N} K_{ij}^{(1)} M_t(j) + \sum_{j=1}^{N} K_{ij}^{(2)} M_z(j) + \sum_{j=1}^{N} K_{ij}^{(3)} J_t(t) + \sum_{j=1}^{N} K_{ij}^{(4)} J_z(j) \quad (9)$$

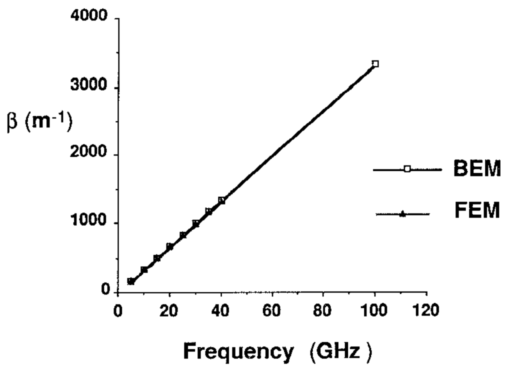

Fig. 2. Comparison of BEM to FEM. Calculation of propagation constant vs. frequency for trapezoid with dimensions: $W_s = 25\,\mu\text{m}, h = 10\,\mu\text{m}, \theta = 35°$ and $\epsilon_r = 3.3$.

$$\frac{1}{2}J_t(i) = \sum_{j=1}^{N} L_{ij}^{(1)} M_t(j) + \sum_{j=1}^{N} L_{ij}^{(2)} M_z(j) + \sum_{j=1}^{N} L_{ij}^{(3)} J_t(t) + \sum_{j=1}^{N} L_{ij}^{(4)} J_z(j) \tag{10}$$

$$\frac{1}{2}M_z(i) = \sum_{j=1}^{N} P_{ij}^{(1)} M_t(j) + \sum_{j=1}^{N} P_{ij}^{(2)} M_z(j) + \sum_{j=1}^{N} P_{ij}^{(3)} J_t(t) + \sum_{j=1}^{N} P_{ij}^{(4)} J_z(j) \tag{11}$$

$$\frac{1}{2}J_z(i) = \sum_{j=1}^{N} Q_{ij}^{(1)} M_t(j) + \sum_{j=1}^{N} Q_{ij}^{(2)} M_z(j) + \sum_{j=1}^{N} Q_{ij}^{(3)} J_t(t) + \sum_{j=1}^{N} Q_{ij}^{(4)} J_z(j) \tag{12}$$

where $K_{ij}^{()}, L_{ij}^{()}$, etc., represent integrals over each subdomain. From these equations, a complex matrix $\overline{\overline{A}}(\beta)$ of dimension $4N$ by $4N$ is formed, with the unknown boundary sources represented as the vector $\overline{x}$

$$\overline{x} = [M_t(1), \cdots, M_t(N), M_z(1), \cdots, M_z(N), J_t(1), \cdots, J_t(N), J_z(1), \cdots, J_z(N)]. \tag{13}$$

This matrix is then solved for the real eigenvalues which correspond to the allowed propagation constants β, i.e.,

$$\overline{\overline{A}}(\beta) \cdot \overline{x} = \emptyset \Rightarrow D = \det[\overline{\overline{A}}(\beta)] = 0. \tag{14}$$

This last step is accomplished by performing a root search for $k_1 \leq \beta \leq k_2$. To avoid a complex root search for a real β, we instead search both real and imaginary parts of D separately. We have found that for the dominant mode, a physical β will be a root of both parts to within some numerical error. Roots that are not common to both parts of D are not solutions of (14) and are discarded.

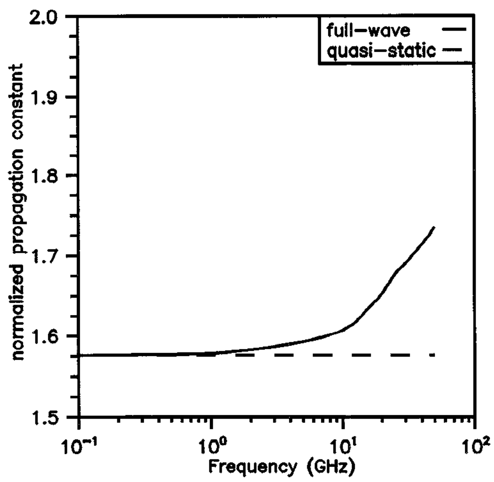

Fig. 3. Calculated normalized propagation constant vs. frequency for the dominant mode of a trapezoid with dimensions: $W_s = 2.5\,\text{mm}, H = 1.0\,\text{mm}, \theta = 35°$, and $\epsilon_r = 3.3$.

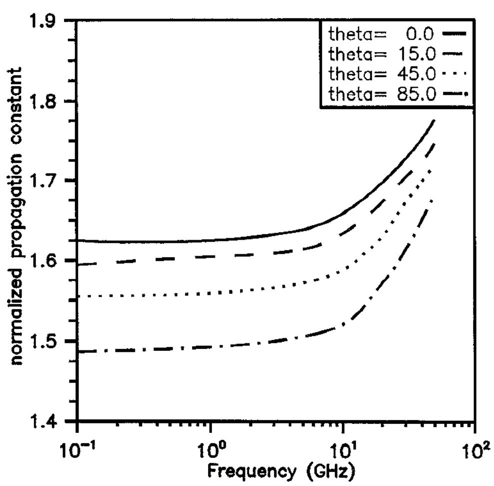

Fig. 4. Comparison of calculated normalized propagation constant versus frequency for the dominant mode of four trapezoids with dimensions: $H = 1.0\,\text{mm}, \epsilon_r = 3.3$, and (a) $\theta = 0.0, W_s = 2.5\,\text{mm}$; (b) $\theta = 15.0, W_s = 2.5\,\text{mm}$; (c) $\theta = 45.0, W_s = 2.35\,\text{mm}$; (d) $\theta = 85\ 0, W_s = 2.52\,\text{mm}$.

Each of equations (5)–(8) [or (9)–(12)] hold for regions 1 or 2. The tangential electric and magnetic fields must be continuous across the dielectric boundaries (i.e., segments ab and cd). This implies that M_t, M_z, J_t, and J_z are continuous, and therefore we have only four unknowns on these boundaries. Along the perfectly conducting strip, J_t and J_z are not continuous ($\hat{n}_1 \times \overline{H}_1 \neq \hat{n}_2 \times \overline{H}_2$), but since M_t, M_z are known (= 0 on the strip), we again have only four unknowns on this portion of the boundary. Hence, along the entire boundary we have four unknowns but we have eight equations. We therefore have several possible combinations that can be used to solve the eigenvalue problem posed in (14). For electrically small structures, we have found that only (11) and (12) produce solutions free of spurious modes. Note that a spurious mode is a root which is common to both real and imaginary parts of D [i.e., a solution of (14)], which does not represent a physical mode. It is possible that this is somehow due to the fact that the dominant currents of this structure should be the M_z, J_z components (which correspond to E_t and H_t respectively), not the M_t, J_t components (which correspond to E_z and H_z). For electrically larger structures (i.e., higher frequencies), all pairwise combinations of (9)–(12) worked equally well, although occasionally spurious solutions were produced. We should note that spurious solutions are also produced when all four equations are combined and solved as in [7]. Fortunately, we could easily identify which solutions are spurious and which is the dominant mode by simply comparing to the quasi-static solution. Obviously, the identification of higher order modes is not as simple.

Once β has been determined, the unknown vector $\overline{x}$ is found from (14) by using singular value decomposition. We therefore obtain the electric and magnetic currents along the boundary. We can then use these in (5)–(8) to obtain the fields anywhere in the cross section by moving the observation point (x', y') off of the boundary and performing a few simple manipulations. A more general and elaborate description of this procedure can be found in [14] and [15].

III. Results

Since this structure has only been recently proposed, there are no results in the literature for which comparisons can be made. Fortunately, we do have calculated design data from a vector FEM program. In Fig. 2 we compare results for β and the characteristic impedance for a trapezoid with $W_s = 25\,\mu\text{m}, H = 10\,\mu\text{m}, \theta = 35°$, and $\epsilon_r = 3.3$ (polyimide). Although the results for β are indistinguishable at the scale shown, there is a 0.6% difference between calculations. We attribute this difference to inaccuracies of both methods in modeling the edge condition. It is also evident from these curves that the propagating mode is quasi-TEM over the frequency range shown.

In Fig. 3 we plot the normalized propagation constant β/k_o versus frequency of the dominant mode for a trapezoid with $W_s = 2.5\,\text{mm}, H = 1.0\,\text{mm}, \theta = 35°$, and $\epsilon_r = 3.3$. Since this structure is electrically larger, the effects of dispersion are evident. In Fig. 4 we compare β/k_o versus frequency for the dominant mode of four trapezoids with angles of $\theta = 0.0, \theta = 15.0, \theta = 45.0$, and $\theta = 85.0$ degrees, and strip widths of $W_s = 2.5, 2.5, 2.35$, and 2.52 mm, respectively. All have $H = 1.0$ mm, and the data for $\theta = 0.0$ were obtained by using a spectral domain program. As θ decreases, the proportion of dielectric to air seen by the dominant mode increases at a given frequency and hence the higher values of β.

IV. Conclusion

We have demonstrated an efficient full wave analysis of a trapezoidal transmission line by the boundary element method. We use an expedient choice of Green's function to reduce the domain of the requisite integral equations, and therefore substantially reduce the amount of computation necessary to solve for the propagation constant. We have found that, in general, all of the integral equations used give spurious solutions, although in some cases they do not appear. In this application, we can readily identify the correct dominant mode, and we have presented data which compare the dispersive properties of a few of these transmission lines.

Acknowledgment

The authors thank ATR for providing data from their FEM calculations, and A. Tran for assisting in data verification. We would also like to thank Dr. B. Young of Hughes RSG for many helpful discussions.

References

[1] H. Nakamoto, T. Hiraoka, and T. Tokumitsu, "Very small multi-layer MMIC hybrids using polyimide films," in *Proc. 3rd Asia-Pacific Microwave Conf.,* Sept. 1990, pp. 1113–1116.
[2] X. Ogawa, X. Hasegawa, X. Banba, and X. Nakamoto, "MMIC transmission lines for multi-layered MMIC's," presented at the 1991 MTT Int. Micro. Symp.
[3] B. Young and T. Itoh, "Analysis and design of Microslab waveguide," *IEEE Trans. Microwave Theory Tech.,* vol. MTT-35, pp. 850–857, Sept. 1987.
[4] M. H. Lean, "Electromagnetic field solution with boundary element method," Ph.D. dissertation, Univ. Manitoba, Winnipeg, Canada, 1980.
[5] S. Kagami and I. Fukai, "Application of boundary element method to electromagnetic field problems," *IEEE Trans. Microwave Theory Tech.,* vol. MTT-32, pp. 455–461, Apr. 1984.
[6] M. Koshiba and M. Suzuki, "Application of the boundary element method to waveguide discontinuities," *IEEE Trans. Microwave Theory Tech.,* vol. MTT-34, pp. 301–307, Feb. 1985.
[7] R. E. Collin and D. A. Ksienski, "Boundary element method for dielectric resonators and waveguides," *Radio Sci.,* vol. 22, no. 7, pp. 1155–1167, Dec. 1987.
[8] S. Schroeder and I. Wolff, "A new hybrid mode boundary integral method for analysis of MMIC waveguides with complicated crossection," in *Proc. IEEE MTT Symp.,* 1989, pp. 711–714.
[9] J. Charles, H. Baudrand, and D. Bajon, "A full-wave analysis of an arbitrarily shaped dielectric waveguide using Green's scalar identity," *IEEE Trans. Microwave Theory Tech.,* vol. MTT-39, pp. 1029–1034, June 1991.
[10] M. McDougall and J. P. Webb, "Infinite elements for the analysis of open dielectric waveguides," *IEEE Trans. Microwave Theory Tech.,* vol. MTT-37, pp. 1724–1731, Nov. 1989.
[11] R. A. Khebi, A. B. Kouki, and R. Mittra, "Higher order asymptotic boundary condition for the finite element modeling of two dimensional transmission line structures," *IEEE Trans. Microwave Theory Tech.,* vol. MTT-38, pp. 1433–1437, Oct. 1990.
[12] R. E. Collin, *Field Theory of Guided Waves,* 2nd ed. New York: IEEE Press, 1991.
[13] C. T. Tai, *Dyadic Green's Functions in Electromagnetic Theory.* Scranton, PA: Intext Educational, 1971.
[14] C. A. Brebbia and S. Walker, *Boundary Element Techniques in Engineering.* London: Newnes-Butterworths, 1980.
[15] E. Yamashita, *Analysis Methods for Electromagnetic Wave Problems.* Norwood, MA: Artech House, 1990.

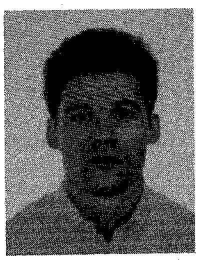

Brent Toland received the B.S. degree in engineering physics from U.C. Berkeley, CA, in 1985, and the M.S.E.E. degree from the University of California, Los Angeles (UCLA) in 1988.

Since 1985 he has been with the Antenna Systems Laboratory at TRW, where he has worked mainly on the analysis and design of satellite antennas. He is currently a Research Assistant at UCLA where he is working toward the Ph.D. degree in electrical engineering.

Tatsuo Itoh (S'69–M'69–SM'74–F'82) received the Ph.D. degree in electrical engineering from the University of Illinois, Urbana, in 1969.

From September 1966 to April 1976, he was with the Electrical Engineering Department, University of Illinois. From April 1976 to August 1977, he was a Senior Research Engineer in the Radio Physics Laboratory, SRI International, Menlo Park, CA. From August 1977 to June 1978, he was an Associate Professor at the University of Kentucky, Lexington. In July 1978 he joined the Faculty at the University of Texas at Austin, where he became a Professor of Electrical Engineering in 1981 and Director of the Electrical Engineering Research Laboratory in 1984. During the summer of 1979, he was a guest researcher at AEG-Telefunken, Ulm, West Germany. In September 1983 he was selected to hold the Hayden Head Centennial Professorship of Engineering at The University of Texas. In September 1984 he was appointed Associate Chairman for Research and Planning of the Electrical and Computer Engineering Department at The University of Texas. In January 1991 he joined the University of California, Los Angeles, as Professor of Electrical Engineering and holder of the TRW Endowed Chair in Microwave and Millimeter Wave Electronics and is Co-Director of Joint Services Electronics Program.

Dr. Itoh is a member of the Institute of Electronics and Communication Engineers of Japan, Sigma Xi, and Commissions B and D of USNC/URSI. He served as the Editor on the IEEE TRANSACTIONS ON MICROWAVE THEORY AND TECHNIQUES for 1983–1985. He serves on the Administrative Committee of IEEE Microwave Theory and Techniques Society. He was Vice President of the Microwave Theory and Techniques Society in 1989 and President in 1990. He is the Editor-in-Chief of the IEEE MICROWAVE AND GUIDED WAVE LETTERS. He also serves on the IEEE TAB Periodicals Council and Publications Board as Division IV Representative for 1992–1993. He was the Chairman of USNC/URSI Commission D from 1988 to 1990, and is the Vice Chairman of Commission D of the International URSI.